Gravity Disturbances, the Marussi Tensor, Invariants and Other Functions of the Geopotential as Represented by the Global Gravity Field Model EGM 2008 and Suggestions for Geo-applications

J. Klokočník [1], J. Kalvoda[4], J. Kostelecký [2,3], A. Bezděk[1], L. V. Eppelbaum[5]

[1] Astronomical Institute, Academy of Sciences of the Czech Republic, CZ-251 65 Ondřejov, Czech Republic, jklokocn@asu.cas.cz, bezdek@asu.cas.cz
[2] Research Institute of Geodesy, Topography and Cartography, CZ-250 66 Zdiby 98, Czech Republic, kost@fsv.cvut.cz
[3] Department of Advanced Geodesy, Czech Technical University, CZ-166 29 Praha 6, Thákurova 7, Czech Republic,
[4] Faculty of Science, Charles University in Prague,CZ-128 43 Praha 2, Albertov 6, Czech Republic, kalvoda@natur.cuni.cz
[5] Department of Geophysical, Atmospheric & Planetary Sciences, Tel Aviv University, Ramat Aviv 69978, Israel, levap@post.tau.ac.il

Presented at ESA Living Planet Symposium,
9 – 13 September, 2013 Edinburgh, UK

Abstract

A new methodology and tools for computing gravity disturbances, the Marussi tensor, invariants of the gravity field, other functionals and functions of the geopotential, as represented by the Global gravity field model EGM 2008 (hereinafter called derivatives), are provided. Regional examples of computed quantities from the EGM 2008 are presented with suggestions of geomorphological and geodynamic interpretations as a motivation for further geo-applications. They are discussed main results obtained for selected regions of the Earth, such as are the Nepal Himalaya and its neighbouring areas, the collision zone of East-Asian and West-Pacific lithospheric plates, the Dead Sea area in Asia Minor, the large impact crater Popigai, and also the Ghawar oil fields in the Saudi Arabia.

Theory

Gravity gradient tensor **Γ** (Marussi tensor) is a tensor of the second derivatives of the disturbing potential V and is computed by means of the harmonic geopotential coefficients (Stokes parameters) C_{lm}, S_{lm} of the particular gravity field model known to maximum degree l_{max} (see details about EGM 2008).

$$\mathbf{\Gamma} = \begin{bmatrix} \Gamma_{11} & \Gamma_{12} & \Gamma_{13} \\ \Gamma_{21} & \Gamma_{22} & \Gamma_{23} \\ \Gamma_{31} & \Gamma_{32} & \Gamma_{33} \end{bmatrix} = - \begin{bmatrix} \frac{\partial^2 T}{\partial x^2} & \frac{\partial^2 T}{\partial x \partial y} & \frac{\partial^2 T}{\partial x \partial z} \\ \frac{\partial^2 T}{\partial y \partial x} & \frac{\partial^2 T}{\partial y^2} & \frac{\partial^2 T}{\partial y \partial z} \\ \frac{\partial^2 T}{\partial z \partial x} & \frac{\partial^2 T}{\partial z \partial y} & \frac{\partial^2 T}{\partial z^2} \end{bmatrix}$$

Outside the source, the potential T satisfies Laplace's equation, the trace of the tensor is zero, **Γ** is symmetric, and contains just five independent components.

Under any coordinate transformation **Γ** contains three invariants

$$\boldsymbol{I_0} = \boldsymbol{trace}\,(\Gamma)$$

$$\boldsymbol{I_1} = \Gamma_{11}\Gamma_{22} + \Gamma_{22}\Gamma_{33} + \Gamma_{33}\Gamma_{11} - \Gamma_{12}^2 - \Gamma_{23}^2 - \Gamma_{13}^2$$

$$\boldsymbol{I_2} = \boldsymbol{det}(\Gamma) = \Gamma_{11}(\Gamma_{22}\Gamma_{33} - \Gamma_{23}^2) + \Gamma_{12}(\Gamma_{23}\Gamma_{13} - \Gamma_{12}\Gamma_{33}) + \Gamma_{13}(\Gamma_{12}\Gamma_{23} - \Gamma_{13}\Gamma_{22})$$

Pedersen and Rasmussen (1990) showed that the invariant ratio $\boldsymbol{I}$ defined as

$$0 \le \boldsymbol{I} = -\frac{(\boldsymbol{I_2}/2)^2}{(\boldsymbol{I_1}/3)^3} \le 1$$

and lies between zero and unity for any potential field. If the causative body is strictly 2D, then $\boldsymbol{I}$ is equal to zero, when the causative body as seen from the observation point looks more and more 3D – like, then $\boldsymbol{I}$ increases and approaches 1.

The strike angle θ_s is determined through

$$\tan 2\theta_s = 2\frac{\Gamma_{12}(\Gamma_{11} + \Gamma_{22}) + \Gamma_{13}\Gamma_{23}}{\Gamma_{11}^2 - \Gamma_{22}^2 + \Gamma_{13}^2 - \Gamma_{23}^2}$$

within a multiple of π/2. Provided that I is small, the strike angle may indicate a dominant 2D structure. For more details see Pedersen and Rasmussen (1990) and Beiki and Pedersen (2010).

Virtual deformation

To define the term "*virtual deformation*", we will utilize an analogy with the tidal deformation. If there is tidal potential T, then horizontal shifts (deformations) exist due to it and they can be expressed as follows in North-South direction (latitude direction)

$$u_\Phi = l_S \frac{1}{g}\frac{\partial T}{\partial \varphi}$$

in East-West direction (longitudinal direction)

$$u_\Lambda = l_S \frac{1}{g\cos\varphi}\frac{\partial T}{\partial \lambda}$$

where g is gravity acceleration 9.81 m.s^{-2}, l_S is the elastic coefficient (Shida number) expressing the elastic properties of the Earth as a whole planet (l_S = 0.08), φ and λ are the geocentric coordinates of a point P where we measure T; the disturbing potential T is in [m^2.s^{-2}]; but in our case, T is represented not tidal, but by **gravity potential**. This mechanism is applied to a standard Earth model (here EGM 2008), but real values of the Shida parameters l for the Earth´s surface are not known.

We apply the apparatus of mechanics of continuum to derive the main directions of the tension. The tensor of deformation $\boldsymbol{E}$ is defined as a gradient of shift. Let us select a local coordinate system *(x,y)* in P by the equations

$$d\varphi = dx, \quad d\lambda \cos\varphi = dy.$$

Then it holds that

$$\boldsymbol{E} = \begin{pmatrix} \epsilon_{11} & \epsilon_{12} \\ \epsilon_{21} & \epsilon_{22} \end{pmatrix} = grad(\mathbf{d}) = \begin{pmatrix} \frac{\partial u_x}{\partial x} & \frac{\partial u_x}{\partial y} \\ \frac{\partial u_y}{\partial x} & \frac{\partial u_y}{\partial y} \end{pmatrix}$$

$$\mathbf{d} = \boldsymbol{E}\,\mathbf{x} + \mathbf{t}$$

where $\boldsymbol{d}$ is the vector of shift, $\boldsymbol{E}$ the gradient of shift, $\boldsymbol{x}$ the vector of the coordinates and $\boldsymbol{t}$ the vector of translation. The tensor of deformation can be separated into two parts:

$$\boldsymbol{E} = \mathbf{e} + \mathbf{\Omega} = (\mathrm{e_{ij}}) + (\Omega_{\mathrm{ij}})$$

where $\boldsymbol{e}$ is the symmetrical tensor and $\boldsymbol{\Omega}$ the anti-symmetrical tensor of deformation, respectively. We will need **e**:

$$\mathbf{e} = \begin{pmatrix} \mathrm{e}_{11} & \mathrm{e}_{12} \\ \mathrm{e}_{21} & \mathrm{e}_{22} \end{pmatrix} = \begin{pmatrix} \epsilon_{11} & (\epsilon_{12} + \epsilon_{21})/2 \\ (\epsilon_{12} + \epsilon_{21})/2 & \epsilon_{22} \end{pmatrix}$$

and the parameters of deformation

$\Delta = e_{11} + e_{22}$ total dilatation
$\gamma_1 = e_{11} - e_{22}$ pure cut
$\gamma_2 = 2e_{12}$ technical cut
$\gamma = (\gamma_1^2 + \gamma_2^2)^{1/2}$ total cut
$a = ½ (\Delta + \gamma)$ major semi-axis of ellipse of deformation
$b = ½ (\Delta - \gamma)$ minor semi-axis of ellipse of deformation
$\alpha = ½\, \mathrm{atan}(\gamma_2 / \gamma_1)$ direction of main axis of deformation.

In relevant sketch maps of complex figures, the semi-axis of deformation ellipse a and b are expressed together with their relative size. Values of l_s are not known, and, therefore, only main directions of the virtual deformations (and not also their amplitudes) are demonstrated. The plotted quantities are a and b expressed in the figures as small crosses.
Virtual deformations of the ellipse of deformation, calculated using the tensor of deformation $\boldsymbol{E}$, are geometrically expressed by its dilatation or compression. Virtual dilatations of the ellipse of deformation indicates

Quality of data and computations

The EGM 2008 (Pavlis et al. 2008 a,b, 2012) is a combined solution (from satellite and terrestrial data) complete to the degree and order 2160 in a spherical harmonic expansion. It also contains additional coefficients extending to the degree 2190 and order 2159. *Satellite data* to the EGM 2008 come only from the GRACE A/B SST (low-low satellite-to-satellite tracking). The *terrestrial data* base of EGM 2008 is very extensive and consists of several sources – gravimetric measurements, anomalies derived from altimetry, models or fill-in data from digital models of the terrain when nothing better was available. EGM 2008 is probably the best currently available combination gravity field model of the Earth. Nevertheless, it does not yield a homogeneous gravity anomaly field. For example, no terrestrial data in EGM 2008 are available for Antarctica. The accuracy and resolution of the derivatives of the EGM 2008 geopotential for some of the mountain belts and other regions with the fill-in data can be several times lower than for the best covered areas.

A note about the units of plotted functionals: *mGal* for the gravity anomalies and/or disturbances, E = Eötvös for the second order potential derivatives. The invariants I_1 and I_2 have units [s^{-4}] and [s^{-6}] and the ratio I is space-less. The strike angle θ_S is expressed in degrees and its demonstration in red means its direction to the East and in blue to the West of the meridian.

Selected results and discussions: aspects of the EGM 2008 in varied regions of the Earth

A systematic screening was performed of correlations between aspects of the geopotential, as represented by the EGM 2008, and large-scale landform patterns displaying varied near-surface geological structures as well as climate-morphogenetic processes. Results of the screening are represented by means of examples from regions of various planation surfaces, high mountain ranges, collision zones of oceanic and continental lithospheric plates, volcanic chains and large impact craters. Selected regions with demonstration of aspects from EGM 2008 are as follows: the Nepal Himalaya and its neighbouring areas, the collision zone of East-Asian and West-Pacific lithospheric plates, the Dead Sea area in Asia Minor an the large impact crater Popigai.

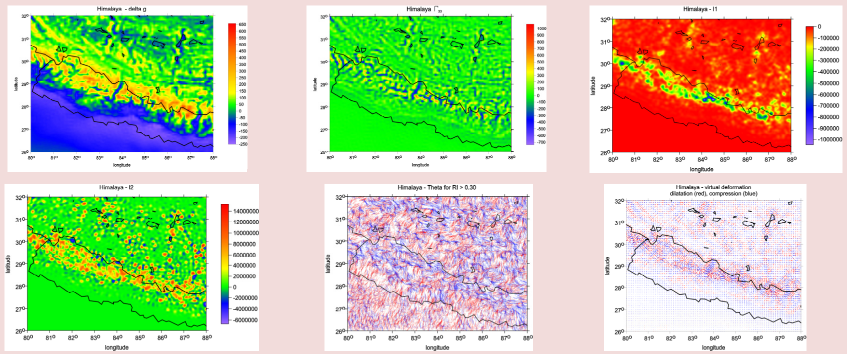

The Nepal Himalaya and its neighbouring regions

Strong coincidences were identified between the large-scale landform configuration of the Himalaya and the extension of regions with very high positive values of the radial second derivative of the disturbing gravitational potential Γ_{33} and the most likely in combination with conspicuous areas of high negative values of Γ_{33} in their close neighbourhood (Kalvoda et al. 2010). Specific configuration and sharp differences in orographical patterns of the Himalaya are indicated by a large range of values of Γ_{33} approximately between +1100 E and –760 E. It is a conspicuous reflection of high mountain massifs divided by large canyon-like valleys of antecedent origin with very active deep-side erosion and related morphogenetic processes.
A comparison of Δg and Γ_{33} records displaying the southern Himalayan foredeep, the Gangetic Plain is also very instructive. Negative gravity anomalies Δg are sensitive to geological structure driven by a long-term subduction of the Indian sub-continent under the Asian continental plate. On the contrary, the second order derivatives Γ reflect the near-surface mass distribution and flat accumulation landforms of the Gangetic Plain and dissected relief of the Siwalik Hills. Mountain ranges of the Himalaya are also demonstrated by the invariants, namely by zones of the significantly negative $\boldsymbol{I_1}$ and positive $\boldsymbol{I_2}$. The eastern directions of the strike angle θ_S are very noticeable in the Gangetic Plain and the Siwalik Hills and its prevailingly western directions in the Himalayan and Tibetan regions. The main patterns of virtual deformations which are presented by dilatations and contractions of the ellipse of deformation, follow the extremely dissected relief of the Himalaya. Virtual dilatations of the ellipse of deformation are concentrated in mountain vaults, and, on the contrary, its virtual contractions indicate strikingly cut-down areas of the mountainous landscape.

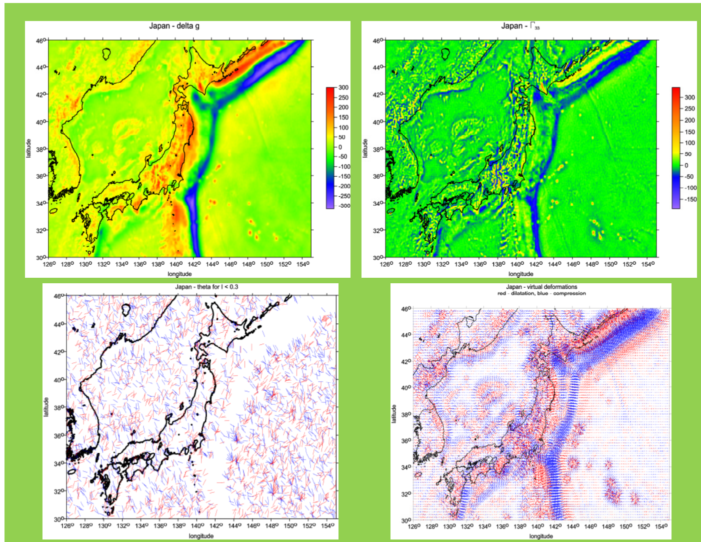

The collision zone of the East-Asian and West-Pacific lithospheric plates

The main large-scale morphostructural patterns of the active collision zone between the Pacific (oceanic) and Asian (continental) plates are quite well expressed by the functionals Δg, Γ_{33} and also partially by strike angle θ_S . Mountain chains of Japanese islands, including the huge massifs of stratovolcanoes, can be determined, especially by the stripes and clusters of positive values of Δg and Γ_{33}. A striking feature drawn is a remarkable arc of deep tectonic trenches connected with the active subduction of the Western-Pacific oceanic plate under the eastern margin of the Asian continental plate. Virtual deformations derived from the ellipse of deformation follow the positions of elevations and depressions of land and submarine reliefs. Demonstrated patterns of these virtual deformations are very similar to the occurrence of gravity anomalies Δg. The topographical features of the Kuril Islands, the Japanese Islands and groups of submarine volcanic massifs in the western part of the Pacific Ocean are especially noticeable, as expressed by positive values of Δg and/or virtual dilatations (compare Figures). The Kuril and Japanese trenches are indicated by negative values of Δg and/or virtual contractions of the ellipse of deformation.

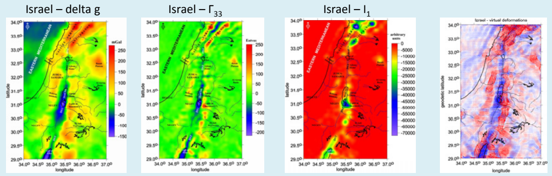

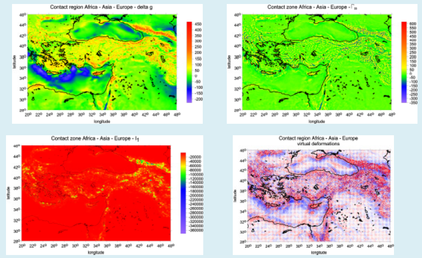

Contact region of north-eastern Africa, south-western Asia, south-eastern Europe and Israel

The complicated geological structure and orographical patterns of the large contact region between these continents can be estimated especially from configurations of highly positive or negative values of Δg, Γ_{33}, I_1 and the virtual deformation. The main orographical patterns including the mountain ranges between the Balkans and the Iranian Highland as well as tectonic basins (e.g. in the Mediterranean Sea west of Cyprus and between Crete and the northern coast of Africa) are conspicuously expressed by Δg and the virtual deformations. Also remarkable are zones with significantly high positive values of Γ_{33} combined with high negative values in close neighbourhoods. It is especially well rendered in regions of the Caucasus and the Elborz mountains as well as the narrow tectonic suture with the Dead Sea.

Analysis for several crystalline tectonic units (terranes) in Israel: Judea-Samaria, Galilee-Lebanon, Antilebanon, Negev, Heletz and Pleshet Basin.
(1) Dead Sea Transform (DST) where strong negative gravity anomalies are caused by thick accumulation of series of low-density sedimentary deposits and salts is clearly detected practically in all gravity maps and their transformants. The evident linear compression zone along the DST is shown by the virtual deformations. (2) Area of Makhtesh Ramon Canyon is characterized by uplift of deep geological associations of heightened density that also is reflected in several maps. (3) A source of Carmel gravity anomaly is uplift of crystallic basement (Eppelbaum and Katz, 2011). (4) Hebron gravity anomaly is produced by high-dense mantle diaper. (5) Basalt plateau in Jordan is reflected in many maps by positive anomaly that is caused by significant difference between density of basalts and surrounding sedimentary deposits. (6) To east of the Dead Sea, some of gravity anomalies may be caused by known uplift of the crystallic basement. (7) The map of the strike angles enables to recognize a dominant location of some subsurface masses and shows very complex distribution of the studied parameters.

.

Area of the Popigai impact crater

The Popigai impact crater (φ = 71°39'N, λ = 111°11'E) in Siberia, with a diameter of about 100 km and age ~35.10^6 years, is partly visible on the surface. According to Klokočník et al. (2010a, b), the Popigai crater is probably not single (compare the second radial derivative Γ_{33}), but double and may be a multiple crater. The virtual deformations of the ellipse of deformation in the Popigai area are displayed, with striking circular structure of the impact crater (virtual compression) surrounded by irregular topographical elevations.

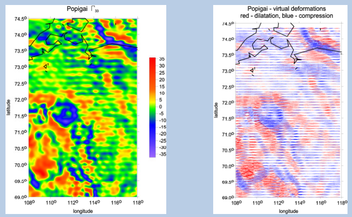

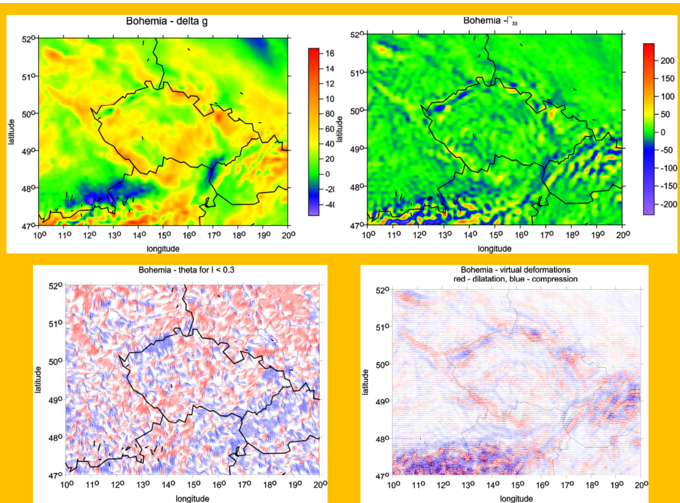

Conspicuous morphotectonic contact between the Bohemian Massif, the Eastern Alps and the Western Carpathians in Central Europe

An example of a varied geological and landform patterns is presented especially in Figures, displaying Δg and Γ_{33} for the Bohemian Massif and its surrounding areas. This part of central Europe includes an extensive region of the geological contact between the Hercynian structures of the Bohemian Massif and the Tertiary Alpine and the Carpathian orogens to the south and/or east of them. A combination of the gravity signatures Δg and Γ_{33} mediates an effective expression of the deeper and near-surface parts of the Earth´s crust and landform patterns. There is a possibility that clusters of western and/or eastern directions of the strike angle θ_S could be a reflection of assumed pressures and tensions in rock massifs of these large morphotectonic units. Figure shows the virtual deformations of the ellipse of deformation with pronounced patterns of mountain belts and highlands (virtual dilatations) and the mainly tectonically conditioned network of valleys and basins (virtual compressions) with active erosion and/or accumulation processes.

Acknowledgments

The paper was completed in the framework of the projects 13-36843S and P209/12/J068 of the Grant Agency of the Czech Republic and with support provided by the European Regional Development Fund (ERDF), project "NTIS - New Technologies for Information Society", European Centre of Excellence, CZ.1.05/1.1.00/02.0090.

Conclusions

Theory of Pedersen & Rasmussen (1990) and Beiki & Pedersen (2010) has been extended and applied in various regions of the Earth, using the global gravity field model EGM 2008, with a resolution ~10 km on the ground. For the first time a global or regional view is offered, not only local or regional view based on airborne gradiometry or classical gravimetry data.
An extensive screening of the gravity signatures computed from EGM 2008 and their comparison with morphotectonic patterns and orographical features on a large scale was realized. It is confirmed that their regional configurations are a consequence of landform evolution and reflections of both former and recent sub-surface geological and climate-morphogenetic processes. Landform patterns with very conspicuous combinations of significantly high positive or negative values of Γ_{33} and significant virtual deformations are under the strong influence of rapid and/or intensive geomorphic processes. These geophysical signatures reflect the regional dynamics of Earth surface evolution as characterised by a very effective integration of tectonic and climate-driven morphogenetic processes.

References

BEIKI, M., PEDERSEN, L. B. (2010): Eigenvector Analysis of Gravity Gradient Tensor to Locate Geologic Bodies, Geophysics, 75, 6, 137–149.
EPPELBAUM, L.V., KATZ, Y.I. (2011) Tectonic-Geophysical Mapping of Israel and eastern Mediterranean: Implication for Hydrocarbon Prospecting. Positioning, 2, 1, 36-54.
KALVODA, J., KLOKOČNÍK, J, KOSTELECKÝ, J. (2010): Regional correlation of the Earth Gravitational Model 2008 with morphogenetic patterns of the Nepal Himalaya, Acta Universitatis Carolinae, Geographica, XLV, 2, 53–78, Prague.
KLOKOČNÍK, J., NOVÁK, P., KOSTELECKÝ, J., WAGNER, C. A. (2010a): Detection of Earth impact craters aided by the detailed global gravitational model EGM 2008. Acta Geodynamica et Geomaterialia, 7, 1 (157), 71–97, Prague.
KLOKOČNÍK, J., KOSTELECKÝ, J., PEŠEK, I., NOVÁK, P., WAGNER, C. A., SEBERA, J. (2010b): Candidates for Multiple Impact Craters? Popigai and Chicxulub as seen by the Global High Resolution Gravitational Field Model EGM08, Solid Earth EGU, 1, 71–83,doi: 10.5194/se-1-71-2010.
PAVLIS, N. K., HOLMES, S. A., KENYON, S. C., FACTOR, J. K. (2008a): EGM2008: An Overview of Its Development and Evaluation, National Geospatial-Intelligence Agency, USA. The International Conference of Gravity, Geoid and Earth Observation 2008, 23th – 27th June, Chania, Crete, Greece.
PAVLIS, N. K., HOLMES, S. A., KENYON, S. C., FACTOR, J. K. (2008b): An Earth Gravitational Model to Degree 2160: EGM2008, EGU General Assembly 2008, 13th – 18th April, Vienna, Austria.
PAVLIS, N. K., HOLMES, S. A., KENYON, S.C., FACTOR, J. K. (2012): The Development and Evaluation of the Earth Gravitational Model 2008 (EGM2008), Journal of Geophysical Research, 117, B04406, doi: 10.1029/2011JB008916.
PEDERSEN, B. D., RASMUSSEN, T. M. (1990): The Gradient Tensor of Potential Field Anomalies: Some implications on data Collection and Data Processing of Maps. Geophysics, 55, #12, 1558–1566.